Phase Transition Width of Connectivity of Wireless Multi-hop Networks in Shadowing Environment

Xiaoyuan Ta*‡, Guoqiang Mao*‡, and Brian D.O. Anderson†§
*School of Electrical and Information Engineering, The University of Sydney
†Research School of Information Sciences and Engineering, Australian National University
‡National ICT Australia Limited[1], Sydney, Australia
§National ICT Australia Limited, Canberra, Australia

***Abstract*—In this paper, we study the well-known phase transition behavior of connectivity in a wireless multi-hop network, but, in contrast to other studies, in a shadowing environment. We consider that a total of n nodes are randomly, independently and uniformly distributed on a unit square in $\Re^2$, each node has a uniform transmission power and any two nodes are directly connected if and only if the power received by one node from the other node, as determined by the log-normal shadowing model, is larger than or equal to a given threshold. We extend the results obtained under the unit disk communication model in previous work to the more realistic log-normal shadowing model, and derive an analytical formula for the *phase transition width* of connectivity for large n. We also demonstrate how our results can be extended to higher dimensional networks and to other channel models.**

I. Introduction

A wireless multi-hop network, e.g. a wireless sensor/ad hoc network, is generally formed by a number of self-organized and decentralized wireless devices which communicate with each other in a peer-to-peer manner over wireless channels. Packets are forwarded through either single hop or multi-hop paths between any pair of source and destination. In such a network, most network functions, e.g. routing, topology control, require the network to be connected [1], [2], [3]. A network is said to be connected iff (if and only if) for any pair of two nodes, there is at least one path between them.

One widely studied property of network connectivity is its phase transition behavior. In a network where nodes are randomly and independently distributed in a bounded area and any two nodes are directly connected iff their Euclidean distance is less than or equal to the transmission range (i.e. *the unit disk communication model*), it has been shown that there exists a threshold in transmission range above which the network is connected with a high probability; and there exists another threshold in transmission range below which the network is connected with a low probability [1], [4], [5]. The *difference* between the two thresholds defines the so-called *phase transition width*. The phase transition width is also known as the *threshold width* in some papers [6]. We will give a more rigorous definition of the phase transition width shortly in Section II. Intuitively, the phase transition width gives an indication on how easy/difficult it is to transform a network that is not connected into a connected network. A good understanding of such a phase transition phenomenon is of practical significance for the design and implementation of wireless multi-hop networks [4], [5], [7], [8].

Previous results regarding the phase transition width of connectivity, e.g. [4], [5], [9], are all derived based on a simple channel model, i.e. the unit disk communication model. The unit disk communication model is based on the path loss phenomenon [10] alone, and assumes that the received signal strength at a receiving node from a transmitting node is only determined by a deterministic function of the Euclidean distance between the two nodes. However, in reality, the received signal strength often shows probabilistic variations induced by shadowing effects that are unavoidably caused by different levels of clutter on the propagation path [10], [11]. To better capture physical reality, one should consider the variations of the received signal strength. It has been shown in [12], [13] that a more accurate modeling of the physical layer is indeed important for better understanding of wireless multi-hop network characteristics. This observation motivates us to investigate the phase transition behavior of connectivity by employing a more realistic channel model.

In this paper, we shall investigate analytically the phase transition width of connectivity based on the *log-normal shadowing model* [10] which can better capture the shadowing effects and is more realistic than the unit disk communication model used in the literature. We derive an analytical formula for calculating the phase transition width of connectivity for large n in $\Re^2$. We also conducted simulations to verify our analytical results. Finally, we present a roadmap for extending our result to higher dimensional networks and to other channel models. These results provide valuable insight into the design and implementation of wireless multi-hop networks.

The rest of this paper is organized as follows. Section II describes the network model and some notations used in later analysis. Section III briefly reviews related work. Section IV presents the main result of the paper on the phase transition width of connectivity for large n in $\Re^2$. Section V presents the roadmap for extending the result to 3-dimensional networks and to other channel models. Finally, Section VI concludes this paper and discusses future work.

[1]National ICT Australia is funded by the Australian Government Department of Communications, Information Technology and the Arts and the Australian Research Council through the *Backing Australia Ability initiative* and the ICT Centre of Excellence Program.

978-1-4244-4148-8/09/$25.00 ©2009
This full text paper was peer reviewed at the direction of IEEE Communications Society subject matter experts for publication in the IEEE "GLOBECOM" 2009 proceedings.

II. Preliminaries

A. Wireless channel model

The wireless received signal strength $P_r(d_{uv})$ between any two nodes u and v has been popularly modeled by a log-normal shadowing model [10], [11], [14]:

$$P_r(d_{uv}) = P_t - PL_0(d_0) - 10\alpha \log_{10} \frac{d_{uv}}{d_0} + Z_\sigma, \quad (1)$$

where $P_r(d_{uv})$ is the received power at a receiving node v from a transmitting node u in dB milliwatts, P_t is the transmitted power of the transmitting node u in dB milliwatts, d_{uv} is the Euclidean distance between nodes u and v, $PL_0(d_0)$ is the reference path loss in dB at a reference distance d_0, α is the path loss exponent which indicates the rate at which the received signal strength decreases with distance, and Z_σ is a zero-mean Gaussian (normal) random variable (in dB) with standard deviation σ (also in dB). The reference path loss $PL_0(d_0)$ is calculated using the free space Friis equation or obtained through field measurements at distance d_0 [10]. In this paper, $PL_0(d_0)$ and d_0 are assumed to be known constants [15], [16]. The value of α depends on the environment and terrain structure and can vary between 2 in free space and 6 in heavily built urban areas. The value of σ is usually larger than zero and can be as high as 12 dB [10].

In addition to the log-normal shadowing model, we shall make three further assumptions in this paper, which are commonly used in the area [11], [16], [14]: α remains constant in the entire network area; σ remains constant for all pairs of nodes in the network; propagation paths are symmetric, i.e. the received power at node v from node u is equal to the received power at node u from node v.

For any two nodes u and v, there exists a wireless link between them (or they are directly connected) iff the received power $P_r(d_{uv})$ is not less than some given threshold P_{th} (also in dB milliwatts), i.e. $P_r(d_{uv}) \geq P_{th}$ [10], [11], [14]. Hence, using Eq. 1, the probability that two random nodes u and v separated by a known distance x are directly connected, denoted as $\mathbb{P}(x)$, is given by

$$\mathbb{P}(x) = Pr\{P_r(x) \geq P_{th}\} = \int_{10\alpha \log_{10} \frac{x}{r}}^{\infty} \frac{1}{\sqrt{2\pi}\sigma} e^{-\frac{t^2}{2\sigma^2}} dt, \quad (2)$$

where

$$r = d_0 10^{\frac{P_t - PL_0(d_0) - P_{th}}{10\alpha}} \quad (3)$$

is the transmission range in the absence of shadowing (i.e. $\sigma = 0$). Note that the unit disk communication model is a special case of the log-normal shadowing model when $\sigma = 0$.

In this paper, we consider that all nodes have the same transmission power P_t. It is clear that the shadowing-free transmission range r is related to the transmission power P_t by Eq. 3. Throughout this paper, we shall investigate the transmission power P_t by investigating r given that P_{th} and α are fixed.

B. Network model

In this paper, we represent a wireless multi-hop network by an undirected graph $G(V,E)$ with a set of vertices $V = V(G)$ and a set of edges $E = E(G)$. Each vertex of the set V uniquely represents a node and each edge of the set E uniquely represents a wireless link, and vice versa. The graph $G(V,E)$ is called the *underlying graph* of the network. In the following, we give a formal definition of the underlying graph, denoted as $G(\mathcal{X}_n, r, \sigma)$, of the network considered in this paper.

Definition 1. Let X_1, X_2,..., X_n be n points which are randomly, independently and uniformly distributed on a unit square in $\Re^2$; let $\mathcal{X}_n = \{X_1, X_2, ..., X_n\}$. The underlying graph $G(\mathcal{X}_n, r, \sigma)$ is an undirected graph having $\mathcal{X}_n$ as its vertex set, and with an edge connecting each pair of vertices X_i and X_j in $\mathcal{X}_n$ with probability $\mathbb{P}(\|X_i - X_j\|)$, where r is given by Eq. 3, σ is the standard deviation of the shadowing in the log-normal shadowing model, function $\mathbb{P}(\cdot)$ is given by Eq. 2 and norm $\|\cdot\|$ means the Euclidean norm.

Remark. Although the network model considered in this paper is built on a unit square, all results developed for a square of unit size can be easily extended to a square of arbitrary size. In fact, by a suitable space rescaling [17], [18], all the properties obtained in this paper can be reformulated [17].

Next, we give a formal definition of the phase transition width of connectivity. Let $\mathbb{P}(n,r)$ denote the probability that the graph $G(\mathcal{X}_n, r, \sigma)$ is connected. Here, we consider that α and σ are any fixed values within their normal ranges, e.g. $\alpha \in [2,6]$, $\sigma \in [0,12]$. It is obvious that $\mathbb{P}(n,r)$ is a strictly monotonically increasing function of r for $0 < \mathbb{P}(n,r) < 1$ in some finite interval of r, and $\mathbb{P}(n,r) = 0$ or 1 outside the interval [4], [5]. Let ζ denote a positive real number. Define

$$r(n,\zeta) := \inf(r > 0 : \ \mathbb{P}(n,r) \geq \zeta), \ \zeta \in (0,1). \quad (4)$$

The *phase transition width* of connectivity over the probability interval $[\zeta, 1-\zeta]$ is then defined as

$$\delta(n,\zeta) := r(n, 1-\zeta) - r(n,\zeta), \ \zeta \in (0, \frac{1}{2}). \quad (5)$$

Henceforth, unless otherwise indicated, the short term phase transition width will be used with ζ being simply understood.

C. Notation

Throughout the paper, we will use standard mathematical notations concerning the asymptotic behavior of functions, i.e., $f(n) = o(g(n))$ or $f(n) \ll g(n)$ if $\frac{f(n)}{g(n)} \to 0$ as $n \to \infty$; $f(n) = O(g(n))$ if there exists a constant c and a value n_0 such that $f(n) \leq c \cdot g(n)$ for all $n \geq n_0$; $f(n) \sim g(n)$ if $\frac{f(n)}{g(n)} \to 1$ as $n \to \infty$ [19]. Symbols "o", "O" and "$\sim$" always apply in the limiting case when $n \to \infty$. Define the notation $(\cdot)_+$ as $y_+ = y$ if $y \geq 0$ and $y_+ = 0$ if $y \leq 0$.

III. Related works

In [7], Krishnamachari *et al.* discussed some examples of network properties that exhibit phase transition behavior, such as connectivity, coordination and probabilistic flooding for

978-1-4244-4148-8/09/$25.00 ©2009
This full text paper was peer reviewed at the direction of IEEE Communications Society subject matter experts for publication in the IEEE "GLOBECOM" 2009 proceedings.

route discovery. The authors then pointed out the significance of understanding phase transitions. In [8], Krishnamachari *et al.* showed that three distributed configuration tasks, viz., partition into coordinating cliques, Hamiltonian cycle formation and conflict-free channel allocation, undergo phase transitions with respect to the transmission range. The authors argued that phase transition analysis is useful in self-configuration of wireless networks. In [20], Aspnes *et al.* demonstrated using simulations the existence of the phase transition phenomenon for localizability of wireless sensor networks.

Goel *et al.* [6] proved that all monotone properties [6], [21] of random geometric graphs have a sharp phase transition width, $\delta(n, \zeta)$, which is bounded in $\Re^d$ $(d = 1,\ 2,\ 3)$ by

$$\delta(n,\zeta) \le \bar{\delta}(n,\zeta) = \begin{cases} O(\log^{1/2}\frac{1}{\zeta}/n^{1/2}), & d = 1 \\ O(\log^{3/4} n/n^{1/2}), & d = 2 \\ O(\log^{1/d} n/n^{1/d}), & d \ge 3 \end{cases} \quad (6)$$

Because Eq. 6 are upper bounds for all monotone properties, they may be quite conservative for some specific monotone properties.

Han *et al.* [4] pointed out that because the results in [6] were derived for a *generic* monotone property, they may be further sharpened for certain *specific* monotone graph properties such as connectivity. The authors improved the results of Goel *et al.* for the property of network connectivity in one and two dimensional spaces, and derived the phase transition width of connectivity for large n, i.e.,

$$\delta(n,\zeta) = \begin{cases} \frac{C(\zeta)}{n} + o(n^{-1}), & d = 1 \\ \frac{C(\zeta)}{2}\sqrt{\frac{1}{\pi n \log n}}(1 + o(1)), & d = 2 \end{cases} \quad (7)$$

where $C(\zeta) = \log(\frac{\log \zeta}{\log(1-\zeta)})$. The results are much sharper than the results given in Eq. 6, which indicates that the results in Eq. 6 are quite conservative for a specific monotone property.

Using the same network model assumption as in [4], we have extended the above result derived by Han *et al.* to a more generic situation, i.e. a generic analytical formula for the phase transition width of k-connectivity for large n and for any fixed integer $k > 0$ in d-dimensional space $(d = 1, 2, 3)$ [5]. The result reduces to Eq. 7 when $d = 1,\ 2$ and $k = 1$.

IV. Phase transition width of connectivity

In this section, we derive the main results on the phase transition width $\delta(n, \zeta)$ of connectivity in $\Re^2$ under the log-normal shadowing model. We have ignored the boundary effect in our derivation as is often done.

First, we present the following proposition which will be used in the proof of later theorem.

Proposition 1. *Consider $G(\mathcal{X}_n, r, \sigma)$ in $\Re^2$ and a real number $\omega \in \Re$. Let r satisfy*

$$r = r_n(\omega) = \sqrt{\frac{\log n + \omega}{\pi n \exp\left(\frac{2\eta^2\sigma^2}{\alpha^2}\right)}}. \quad (8)$$

Ignoring the boundary effect, the following holds:

$$\lim_{n\to\infty} \mathbb{P}(n, r_n(\omega)) = \exp\left(-e^{-\omega}\right).$$

Proof: In order to prove the result, we make use of some results derived in [3]. For any wireless channel model $\mathcal{C}$, let $G(\mathcal{X}_n, \mathcal{C})$ denote the undirected graph in $\Re^2$ having $\mathcal{X}_n$ as its vertex set, and with an edge connecting each pair of vertices X_i and X_j in $\mathcal{X}_n$ with probability $g^{\mathcal{C}}(\|X_i - X_j\|)$. Let $\psi(\mathcal{C})$ denote the probability that any two randomly selected vertices in graph $G(\mathcal{X}_n, \mathcal{C})$ are directly connected. Lemmas 1 and 3 in [3] indicate that if $\psi(\mathcal{C}) = \frac{\log n + \omega}{n}$ and $g^{\mathcal{C}}(x)$ satisfies the following conditions of rotational and translation invariance, monotonicity and integral boundedness:

$$\begin{cases} g^{(\mathcal{C})}(x) = g^{(\mathcal{C})}(y) \quad whenever \quad x = y; \\ g^{(\mathcal{C})}(x) \le g^{(\mathcal{C})}(y) \quad whenever \quad x \ge y; \\ \quad 0 < \int_{\Re^2} g^{(\mathcal{C})}(x)dx < \infty, \end{cases} \quad (9)$$

then,

$$\lim_{n\to\infty} Pr\{G(\mathcal{X}_n, \mathcal{C})\ is\ connected\} = \exp\left(-e^{-\omega}\right).$$

It can be easily shown that the log-normal shadowing model satisfies the conditions given by Eq. 9 [3].

It therefore remains to demonstrate that the probability $\psi(\mathcal{C})$ for the log-normal shadowing model, denoted as $\psi(\mathcal{X}_n, r, \sigma)$, assumes the form $\frac{\log n + \omega}{n}$ when r is given by Eq. 8. Let X be the random variable representing the Euclidean distance between two randomly selected nodes in the graph $G(\mathcal{X}_n, r, \sigma)$. Because nodes are uniformly and independently distributed in a unit square, if the boundary effect is ignored, the probability density function (*pdf*) of X, is given by [14]

$$p_X(x) = 2\pi x. \quad (10)$$

Hence, from Eq. 1, Eq. 3 and Eq. 10, we have

$$\begin{aligned} \psi(\mathcal{X}_n, r, \sigma) &= Pr\{P_r(X) \ge P_{th}\} \\ &= Pr\{Z_\sigma \ge 10\alpha \log_{10} \frac{X}{r}\} \\ &= \int_{-\infty}^{\infty} Pr\{X \le r\exp(\frac{\eta z}{\alpha})\} \frac{1}{\sqrt{2\pi}\sigma} e^{-\frac{z^2}{2\sigma^2}} dz. \end{aligned}$$

From Eq. 8, we have $r \to 0$ as $n \to \infty$. Hence, $\min\{1, r\exp(\frac{\eta z}{\alpha})\} = r\exp(\frac{\eta z}{\alpha})$ when $n \to \infty$. Thus, the last equation becomes

$$\begin{aligned} \psi(\mathcal{X}_n, r, \sigma) &\sim \int_{-\infty}^{\infty} \left[\int_0^{re^{\frac{\eta z}{\alpha}}} p_X(x)dx\right] \frac{1}{\sqrt{2\pi}\sigma} e^{-\frac{z^2}{2\sigma^2}} dz \\ &= \int_{-\infty}^{\infty} \left[\int_0^{re^{\frac{\eta z}{\alpha}}} 2\pi x dx\right] \frac{1}{\sqrt{2\pi}\sigma} e^{-\frac{z^2}{2\sigma^2}} dz \\ &= \pi r^2 \exp\left(\frac{2\eta^2\sigma^2}{\alpha^2}\right), \quad as \quad n \to \infty. \end{aligned} \quad (11)$$

Since the log-normal shadowing model satisfies Eq. 9, and Eq. 8 and Eq. 11 imply that $\psi(\mathcal{X}_n, r, \sigma) = \frac{\log n + \omega}{n}$, the result follows by using Lemmas 1 and 3 of [3]. ■

978-1-4244-4148-8/09/$25.00 ©2009
This full text paper was peer reviewed at the direction of IEEE Communications Society subject matter experts for publication in the IEEE "GLOBECOM" 2009 proceedings.

Using the above Proposition 1, the following theorem regarding $r(n,\zeta)$ defined in Eq. 4 can be obtained.

Theorem 1. *Consider $G(\mathcal{X}_n, r, \sigma)$ in $\Re^2$ and a real number $\zeta \in (0,1)$. Ignore the boundary effect. Then, for large n,*

$$r(n,\zeta) = \sqrt{\frac{\log n}{\pi n \exp\left(\frac{2\eta^2\sigma^2}{\alpha^2}\right)}} - \frac{\log\left(\log\left(\frac{1}{\zeta}\right)\right)(1+o(1))}{2\sqrt{\pi n \log n \exp\left(\frac{2\eta^2\sigma^2}{\alpha^2}\right)}}.$$

Proof: For any $\omega \in \Re$, Proposition 1 immediately yields

$$\lim_{n\to\infty} \mathbb{P}(n, r_n(\omega)) = \exp(-e^{-\omega}). \tag{12}$$

Define $\mathcal{Q} := \exp\left(\frac{2\eta^2\sigma^2}{\alpha^2}\right)$, which is considered to be fixed throughout this proof. For each $x \in \Re$, define a $[0,1]$-valued sequence $\{\theta_n(x), n = 1,2,3...\}$ by

$$\theta_n(x) := \min\left(1, \sqrt{\left(\frac{\log n + x}{\mathcal{Q}\pi n}\right)_+}\right),\ n = 1,2,... \tag{13}$$

Because for any fixed $x \in \Re$, $\frac{\log n + x}{\mathcal{Q}\pi n} \to 0$ as $n \to \infty$, there exists a finite integer $N(x)$ such that

$$0 < \sqrt{\frac{\log n + x}{\mathcal{Q}\pi n}} < 1, \quad \forall n > N(x).$$

Hence, we have

$$\theta_n(x) = \sqrt{\frac{\log n + x}{\mathcal{Q}\pi n}}, \quad \forall n > N(x). \tag{14}$$

Therefore, from Proposition 1 and Eq. 12, we have

$$\lim_{n\to\infty} \mathbb{P}(n, \theta_n(x)) = \exp(-e^{-x}). \tag{15}$$

Now fix x in $\Re$, from Eq. 15, we can obtain that for each $\varepsilon > 0$, there exists a finite integer $N(\varepsilon, x)$ such that

$$\left|\mathbb{P}(n,\theta_n(x)) - \exp(-e^{-x})\right| < \varepsilon, \ \ \forall n > N(\varepsilon, x). \tag{16}$$

It can be easily checked that the mapping $\Re \to \Re_+ : x \to \exp(-e^{-x})$ is strictly monotonically increasing and continuous with $\lim_{x\to-\infty}\exp(-e^{-x}) = 0$ and $\lim_{x\to\infty}\exp(-e^{-x}) = 1$. Therefore, for each $\zeta \in (0,1)$, there exists a unique value of x in $\Re$, denoted as x_ζ, such that $\exp(-e^{-x_\zeta}) = \zeta$. In fact, from the equality $\exp(-e^{-x_\zeta}) = \zeta$, we have

$$x_\zeta = -\log(-\log\zeta). \tag{17}$$

Hence, fixing x in $\Re$ is equivalent to fixing ζ in $(0,1)$. Now fix ζ in the interval $(0,1)$, and let ε be sufficiently small such that $0 < 2\varepsilon < \zeta$ and $\zeta + 2\varepsilon < 1$. Then applying Eq. 16 with $x = x_{\zeta+\varepsilon}$ and $x = x_{\zeta-\varepsilon}$ respectively, we have

$$\left|\mathbb{P}(n,\theta_n(x_{\zeta+\varepsilon})) - \exp(-e^{-x_{\zeta+\varepsilon}})\right| < \varepsilon,\ \forall n > N(\varepsilon, x_{\zeta+\varepsilon}) \tag{18}$$

and

$$\left|\mathbb{P}(n,\theta_n(x_{\zeta-\varepsilon})) - \exp(-e^{-x_{\zeta-\varepsilon}})\right| < \varepsilon,\ \forall n > N(\varepsilon, x_{\zeta-\varepsilon}). \tag{19}$$

We always assume that n is sufficiently large when necessary. In the rest of this proof, we assume that $n > N(\varepsilon,\zeta)$ with

$$N(\varepsilon,\zeta) = \max\{N(x_\zeta),\ N(\varepsilon, x_{\zeta+\varepsilon}),\ N(\varepsilon, x_{\zeta-\varepsilon})\},$$

where $N(x_\zeta)$ represents the finite integer above which Eq. 14 holds.

Since $\exp(-e^{-x_{\zeta\pm\varepsilon}}) = \zeta \pm \varepsilon$, it can be readily obtained from Eq. 18 and Eq. 19 that

$$\zeta < \mathbb{P}(n, \theta_n(x_{\zeta+\varepsilon})) < \zeta + 2\varepsilon$$

and

$$\zeta - 2\varepsilon < \mathbb{P}(n, \theta_n(x_{\zeta-\varepsilon})) < \zeta.$$

According to the definition of $r(n,\zeta)$, we have $\mathbb{P}(n, r(n,\zeta)) = \zeta$. Hence, from the last two inequalities, it follows that

$$\mathbb{P}(n, \theta_n(x_{\zeta-\varepsilon})) < \mathbb{P}(n, r(n,\zeta)) < \mathbb{P}(n, \theta_n(x_{\zeta+\varepsilon})).$$

Because of the strict monotonicity of the mapping $r \to \mathbb{P}(n,r)$, we have

$$\theta_n(x_{\zeta-\varepsilon}) < r(n,\zeta) < \theta_n(x_{\zeta+\varepsilon}). \tag{20}$$

Define $\kappa(n,\zeta) := r(n,\zeta) - \theta_n(x_\zeta)$, then it can be obtained from Eq. 20 that

$$\theta_n(x_{\zeta-\varepsilon}) - \theta_n(x_\zeta) < \kappa(n,\zeta) < \theta_n(x_{\zeta+\varepsilon}) - \theta_n(x_\zeta). \tag{21}$$

For any fixed $x \in \Re$, it is clear that

$$\lim_{n\to\infty} \frac{x}{\log n} = 0.$$

Hence, from Eq. 14, we have

$$\begin{aligned}\theta_n(x) &= \sqrt{\frac{\log n}{\mathcal{Q}\pi n}} \times \sqrt{1 + \frac{x}{\log n}} \\ &= \sqrt{\frac{\log n}{\mathcal{Q}\pi n}} \times \left(1 + \frac{1}{2}\frac{x(1+o(1))}{\log n}\right),\ as\ n \to \infty.\end{aligned}$$

Therefore, for any $\zeta \in (0,1)$, we have

$$\begin{aligned}&\theta_n(x_{\zeta\pm\varepsilon}) - \theta_n(x_\zeta) \\ =\ &\frac{x_{\zeta\pm\varepsilon} - x_\zeta}{2\sqrt{\mathcal{Q}\pi n \log n}}(1+o(1)), as\ n \to \infty.\end{aligned} \tag{22}$$

Because Eq. 21 holds for all $n > N(\varepsilon,\zeta)$, it must be valid when $n \to \infty$ as well. And as $n \to \infty$, the small order part $o(1)$ in Eq. 22 goes to zero. Hence, from Eq. 21 and Eq. 22, we have

$$x_{\zeta-\varepsilon} - x_\zeta \ \leq\ \liminf_{n\to\infty}\left(2\sqrt{\mathcal{Q}\pi n\log n} \times \kappa(n,\zeta)\right) \tag{23}$$

$$x_{\zeta+\varepsilon} - x_\zeta \ \geq\ \limsup_{n\to\infty}\left(2\sqrt{\mathcal{Q}\pi n\log n} \times \kappa(n,\zeta)\right) \tag{24}$$

Because ε can be chosen to be arbitrarily small, and as stated earlier $x_\zeta = -\log(-\log\zeta)$ is a continuous and strictly monotonically increasing function of ζ for $\zeta \in (0,1)$, it is evident that

$$\lim_{\varepsilon\downarrow 0}(x_{\zeta-\varepsilon} - x_\zeta) = \lim_{\varepsilon\downarrow 0}(x_{\zeta+\varepsilon} - x_\zeta) = 0. \tag{25}$$

Hence, from Eq. 23, Eq. 24 and Eq. 25, we have

$$\lim_{n\to\infty}\left(2\sqrt{\mathcal{Q}\pi n\log n}\times\kappa(n,\zeta)\right)=0. \tag{26}$$

Thus, given that Eq. 26 holds, it must be true that

$$\kappa(n,\zeta)=o\left(\frac{1}{2\sqrt{\mathcal{Q}\pi n\log n}}\right).$$

Hence, we have

$$\begin{aligned} r(n,\zeta) &= \theta_n(x_\zeta)+\kappa(n,\zeta) \\ &= \sqrt{\frac{\log n}{\mathcal{Q}\pi n}}\left(1+\frac{x_\zeta(1+o(1))}{2\log n}\right)+o\left(\frac{1}{2\sqrt{\mathcal{Q}\pi n\log n}}\right) \\ &= \sqrt{\frac{\log n}{\mathcal{Q}\pi n}}-\frac{\log\left(\log\left(\frac{1}{\zeta}\right)\right)(1+o(1))}{2\sqrt{\mathcal{Q}\pi n\log n}}. \end{aligned}$$

Substituting $\mathcal{Q}=\exp\left(\frac{2\eta^2\sigma^2}{\alpha^2}\right)$ into the last equality, the result follows. Note that some parts of the proof used here are similar to the arguments used in [5]. ■

Comparing $r(n,\zeta)$ in Theorem 1 derived under the log-normal shadowing model with corresponding result derived under the unit disk communication model in [4], [5], we can see that the only difference between them is the exponential term $\exp\left(\frac{2\eta^2\sigma^2}{\alpha^2}\right)$ induced by the shadowing effects. When $\sigma=0$, this exponential term becomes one and the difference vanishes. In reality, $\sigma>0$, and this exponential term is always larger than one, which indicates that less transmission power is needed in a shadowing environment ($\sigma>0$) than in a non-shadowing environment ($\sigma=0$) to obtain a connected network with probability $(1-\zeta)$. Thus, the random variation associated with the log-normal shadowing model is actually helpful in improving network connectivity.

By Theorem 1, the phase transition width $\delta(n,\zeta)$ for large n can be derived in the following Corollary 1.

Corollary 1. *Consider $G(\mathcal{X}_n,r,\sigma)$ in $\Re^2$ and a real number $\zeta\in(0,\frac{1}{2})$. Ignore the boundary effect. Then, for large n,*

$$\delta(n,\zeta)=\frac{\log\left(\frac{\log\zeta}{\log(1-\zeta)}\right)}{2\sqrt{\pi n\log n\exp\left(\frac{2\eta^2\sigma^2}{\alpha^2}\right)}}(1+o(1)). \tag{27}$$

Proof: Since $\delta(n,\zeta)=r(n,1-\zeta)-r(n,\zeta)$ by Eq. 5, $\delta(n,\zeta)$ for large n can be easily obtained by Theorem 1. ■

The only difference between Eq. 27 derived under the log-normal shadowing model and Eq. 7 derived under the unit disk communication model is still $\exp\left(\frac{2\eta^2\sigma^2}{\alpha^2}\right)$. Hence, the phase transition width $\delta(n,\zeta)$ of connectivity is narrower in a shadowing environment ($\sigma>0$) than in a non-shadowing environment ($\sigma=0$).

A. Simulations

In this sub-section, we report simulations conducted to validate the theoretical analysis. We programmed a tool in C++ for the simulations. In the simulations, we consider that a total of n nodes are randomly and uniformly distributed in a unit square in $\Re^2$ and all nodes have the same transmission power. We have used the *toroidal distance metric* [1], [5] to remove the impact of the boundary effect on the simulation results. Because simulations become very computationally intensive and time consuming for large values of n, we limited n to 1500 in the simulations.

Fig. 1 and Fig. 2 show the analytical results and the simulation results for $\delta(n,\zeta)$ in $\Re^2$ with $\zeta=0.4$ and $\zeta=0.05$ respectively. The value of n is varied between 100 and 1500, ζ is set to two typical values, i.e., 0.4 (close to 0.5) and 0.05 (close to 0). When calculating the analytical results by Eq. 27, the small order part is omitted, i.e. $o(1)$ in the term $(1+o(1))$ is ignored. We can see that $\delta(n,\zeta)$ decreases as n grows, which is consistent with Corollary 1. The discrepancy between the analytical results and the simulation results is due to the omission of the small order part $o(1)$ when computing the analytical results. The small order part $o(1)$ is significant when n is small, but it will go to zero as $n\to\infty$. We can also see that $\delta(n,\zeta)$ is smaller for the log-normal shadowing model ($\sigma>0$) than for the unit disk communication model ($\sigma=0$), which is implied by Eq. 27 and Eq. 7. This comparison also accords with the discussion after Corollary 1.

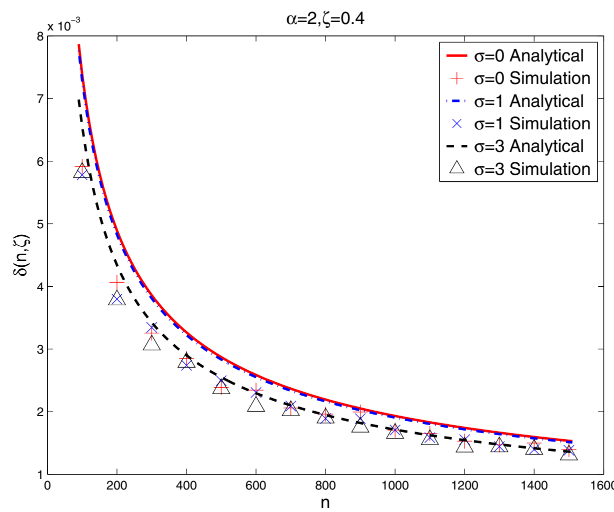

Fig. 1. Phase transition width of connectivity $\delta(n,\zeta)$ *versus* n in $\Re^2$. The value of α is set to 2, and the value of ζ is set to 0.4.

V. 3-DIMENSIONAL NETWORKS AND ARBITRARY CHANNEL MODELS

The analysis and derivation in Section IV provides an efficient roadmap for extending results in this paper to 3-dimensional networks and to other channel models satisfying Eq. 9. In this section, we briefly explain this roadmap.

The principle of the roadmap is to first derive a result comparable to Proposition 1 for 3-dimensional networks or for other channel models, and then apply the same technique used in the proof of Theorem 1 to derive corresponding results comparable to Theorem 1 and Corollary 1.

The results in [3] used for deriving Proposition 1, i.e. Lemmas 1 and 3, are also valid in 3-dimensional networks

This full text paper was peer reviewed at the direction of IEEE Communications Society subject matter experts for publication in the IEEE "GLOBECOM" 2009 proceedings.

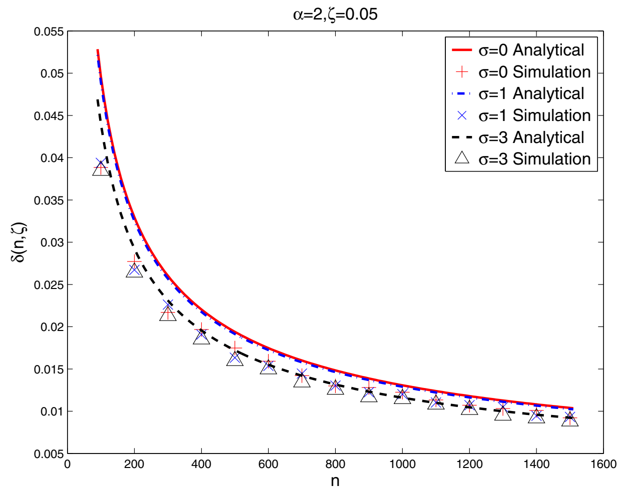

Fig. 2. Phase transition width of connectivity $\delta(n,\zeta)$ *versus* n in $\Re^2$. The value of α is set to 2, and the value of ζ is set to 0.05.

if the node distribution is the same as in this paper and the channel model satisfies Eq. 9. Note that the integral space in Eq. 9 should be changed accordingly from $\Re^2$ to $\Re^3$. Hence, the extension of Theorem 1 and Corollary 1 to 3-dimensional networks and any arbitrary channel model $\mathcal{C}$ satisfying Eq. 9 can be achieved according to the following four steps:

1) Derive the probability $\mathbb{P}^{\mathcal{C}}(x)$ that any two nodes separated by Euclidean distance x are directly connected under the given channel model $\mathcal{C}$. Note $\mathbb{P}(x)$ given by Eq. 2 is the probability derived under the log-normal shadowing model.
2) Derive the *pdf* of the Euclidean distance X between two randomly selected nodes in 3-dimensional space, denoted it as $p_X^{\Re^3}(x)$. Note $p_X(x)$ given by Eq. 10 is the *pdf* derived for 2-dimensional space.
3) Derive $r_n^{\Re^3,\mathcal{C}}(\omega)$ (comparable to $r_n(\omega)$ in Eq. 8), such that the probability that the underlying network with $r_n^{\Re^3,\mathcal{C}}(\omega)$ is connected tends to $\exp\left(-e^{-\omega}\right)$ as $n \to \infty$. It can be obtained using $\mathbb{P}^{\mathcal{C}}(x)$ and $p_X^{\Re^3}(x)$ in the same way as shown in the proof of Proposition 1.
4) Derive corresponding results comparable to Theorem 1 and Corollary 1 using $r_n^{\Re^3,\mathcal{C}}(\omega)$ in the same way as shown in the proofs of Theorem 1 and Corollary 1.

VI. Conclusions and Future Work

In this paper, we extended the well-known result on phase transition width of connectivity obtained under the unit disk communication model to the log-normal shadowing model which is more realistic than the previous one. For large n, we derived an analytical formula for calculating the phase transition width of connectivity in $\Re^2$. We also presented simulations conducted to verify the accuracy of the theoretical analysis. Finally, we provided an efficient roadmap for extending our results to 3-dimensional networks and to other wireless channel models. These results are very useful in the design, self-configuration, and transmission power control in wireless sensor/ad hoc networks.

One direction of our future work is to investigate the phase transition width of k-connectivity ($k > 1$) [5] in a shadowing environment, since we only considered connectivity (or 1-connectivity) in this paper. Another direction is to study the phase transition width considering the boundary effect.

References

[1] C. Bettstetter, "On the Minimum Node Degree and Connectivity of a Wireless Multihop Network," in *3rd ACM International Symposium on Mobile Ad Hoc Networking and Computing*, Lausanne, 2002, pp. 80–91.

[2] F. Xue and P. Kumar, "The number of neighbors needed for connectivity of wireless networks," *Wireless Networks*, vol. 10, no. 2, pp. 169–181, 2004.

[3] X. Ta, G. Mao, and B. D. O. Anderson, "On the Connectivity of Wireless Multi-hop Networks with Arbitrary Wireless Channel Models," *IEEE Communications Letters*, vol. 13, no. 3, pp. 1–3, 2009.

[4] G. Han and A. M. Makowski, "Poisson convergence can yield very sharp transitions in geometric random graphs," in *the Inaugural Workshop, Information Theory and Applications*, San Diego (CA), February, 2006.

[5] X. Ta, G. Mao, and B. D. O. Anderson, "Phase Transition Properties in K-connected Wireless Multi-hop Networks," in *the 51th IEEE Globecom'08*, New Orleans, USA, November, 2008, pp. 1–6.

[6] A. Goel, S. Rai, and B. Krishnamachari, "Sharp Threshold For Monothone Properties In Random Geometric Graphs," in *STOC'04*, Chicago, June, 2004.

[7] B. Krishnamachari, S. B. Wicker, and R. Bejar, "Phase transition phenomena in wireless ad hoc networks," in *IEEE Globecom*, vol. 5, 2001, pp. 2921–2925.

[8] B. Krishnamachari, S. Wicker, R. Bejar, and C. Fernandez, "On the Complexity of Distributed Self-Configuration in Wireless Networks," *Telecommunication Systems*, vol. 22, no. 1-4, pp. 33–59, 2003.

[9] U. N. Raghavan, H. P. Thadakamalla, and S. Kumara, "Phase Transition and Connectivity in Distributed Wireless Sensor Networks," in *13th International Conference on Advanced Computing and Communications*, Coimbatore, India, December, 2005.

[10] T. S. Rappaport, *Wireless Communications: Principles and Practice*, 1st ed. New Jersey: Prentice Hall PTR, 1996.

[11] C. Bettstetter and C. Hartmann, "Connectivity of Wireless Multihop Networks in a Shadow Fading Environment," *Wireless Networks*, vol. 11, no. 5, pp. 571–579, September, 2005.

[12] M. Zorzi and S. Pupolin, "Optimum transmission ranges in multihop packet radio networks in the presence of fading," *IEEE Transactions on Communication*, vol. 43, no. 7, pp. 2201–2205, July, 1995.

[13] M. Takai, J. Martin, and R. Bagrodia, "Effects of wireless physical layer modeling in mobile ad hoc networks," in *ACM Intern. Symp. on Mobile Ad Hoc Netw. and Comp. (MobiHoc)*, Long Beach, USA, October, 2001.

[14] S. Mukherjee and D. Avidor, "Connectivity and Transmit-Energy Considerations Between Any Pair of Nodes in a Wireless Ad Hoc Network Subject to Fading," *IEEE Transactions on Vehicular Technology*, vol. 57, no. 2, pp. 1226–1242, March, 2008.

[15] N. Patwari, A. O. Hero, M. Perkins, N. S. Correal, and R. J. ODea, "Relative location estimation in wireless sensor networks," *IEEE Transactions on Signal Processing*, vol. 51, no. 8, pp. 2137–2148, 2003.

[16] G. Mao, B. D. O. Anderson, and B. Fidan, "Path loss exponent estimation for wireless sensor network localization," *Computer Networks*, vol. 51, no. 10, pp. 2467–2483, July, 2007.

[17] M. Penrose, *Random Geometric Graphs*, 1st ed. Oxford: Oxford University Press, 2003.

[18] R. Meester and R. Roy, *Continuum Percolation*. Cambridge, UK: Cambridge University Press, 1996.

[19] N. G. D. Bruijn, *Asymptotic Methods in Analysis*, 2nd ed. New York: Dover Publications, Inc., 1981.

[20] J. Aspnes, T. Eren, D. K. Goldenberg, A. S. Morse, W. Whiteley, Y. R. Yang, B. D. O. Anderson, and P. N. Belhumeur, "A Theory of Network Localization," *IEEE Transactions on Mobile Computing*, vol. 5, no. 12, pp. 1663–1678, December, 2006.

[21] S. Janson, T. Luczak, and A. Rucinski, *Random Graphs*, 1st ed. New York: John Wiley and Sons, 2000.